



Thermoanalytical study and crystallization of Ba(PO₃)₂–WO₃ glasses

Petr Kalenda¹ · Ladislav Koudelka¹ · Petr Mošner¹ · Ludvík Beneš² · Helena Drobná³

Received: 21 August 2018 / Accepted: 15 February 2019 / Published online: 2 March 2019

© Akadémiai Kiadó, Budapest, Hungary 2019

Abstract

Barium phosphate glasses of the composition (100 – x)Ba(PO₃)₂–xWO₃ with 0–60 mol% WO₃ were prepared and studied. Thermal studies of the glasses were carried out with DTA, dilatometry and hot-stage microscopy. Glass transition temperature in this glass series increases with increasing WO₃ content from 461 °C (x = 0) to 623 °C (x = 60). Most glasses containing WO₃ crystallize on heating within the range of 650–750 °C with the exception of glasses with 20–30 mol% WO₃, which are thermally stable. Very high chemical durability of these glasses with dissolution rate of 1.4 × 10^{–8}–6.2 × 10^{–9} g cm^{–2} min^{–1} was also revealed. Crystallization of glasses revealed the existence of a new compound Ba(WO₂)₂(PO₄)₂ in the studied compositional series. The compound Ba(WO₂)₂(PO₄)₂ possess hexagonal unit cell of dimensions *a* = 11.5191(1) Å and *c* = 6.3437(1) Å, and its melting point is 936 °C. Raman spectra of crystallized glasses confirmed the formation of crystalline compound in this glass series and revealed the presence of glass phase in some thermal-treated samples. ³¹P MAS NMR showed on only one coordination of phosphorus atoms in the Ba(WO₂)₂(PO₄)₂ compound.

Keywords Phosphate glasses · Thermal properties · Physical properties · Crystallization

Introduction

Phosphate glasses rank among materials with many interesting properties for technological applications such as low melting temperature, low glass transition temperature or high transparency for ultraviolet light, but with relatively poor chemical durability [1]. This problem can be solved by modifying these glasses with transition metal oxides (TM), such as Fe₂O₃, Nb₂O₅, MoO₃ or WO₃ [2, 3]. Phosphate glasses modified with tungsten oxide exhibit

also interesting electrochromic and photochromic properties applicable in special optical materials [4, 5].

NaPO₃–WO₃ glasses were studied by de Araujo et al. [6]. From structural studies with solid-state NMR and Raman spectroscopy, the authors [6] claim that tungsten oxide forms WO₆ octahedra interlinking metaphosphate chains based on PO₄ tetrahedra. According to [6], in the glasses containing more than 40 mol% WO₃ the majority of phosphorus atoms is present as P(OW)₄ tetrahedra. Glasses of AgPO₃–WO₃ series were studied by Santagneli et al. [7]. The authors [7] confirmed the formation of P–O–W connectivities and their XANES measurements showed on the formation of octahedrally coordinated tungsten. The blue color of tungsten phosphate glasses is caused by the presence of W⁵⁺ ions in the glass [8]. The study of thermal properties of tungstate-phosphate glasses [9–11] showed the increase in glass transition temperature with increasing WO₃ content.

The experimental data on barium tungstate-phosphate glasses are scarce. The available data on these glasses are from X-ray absorption study in [12], where the authors studied distortion of WO₆ octahedra in three glasses of Ba(PO₃)₂–WO₃ series. Marzouk et al. [13] studied barium metaphosphate glasses modified by WO₃ with the application of optical, FTIR and ESR spectroscopies, but this

Electronic supplementary material The online version of this article (<https://doi.org/10.1007/s10973-019-08115-w>) contains supplementary material, which is available to authorized users.

✉ Petr Kalenda
petr.kalenda2@upce.cz

¹ Department of General and Inorganic Chemistry, Faculty of Chemical Technology, University of Pardubice, 532 10 Pardubice, Czech Republic

² Joint Laboratory of Solid State Chemistry, University of Pardubice, 532 10 Pardubice, Czech Republic

³ Department of Physical Chemistry, Faculty of Chemical Technology, University of Pardubice, 532 10 Pardubice, Czech Republic

study is devoted to the glasses with the addition of only 0–3 mass% WO_3 .

The aim of the present work was the investigation of thermal behavior and physico-chemical properties of $(100 - x)\text{Ba}(\text{PO}_3)_2 - x\text{WO}_3$ glasses. Their crystallization was studied by thermoanalytical methods, and crystallization products were analyzed with X-ray diffraction and Raman spectroscopy. Glasses with barium oxide, instead of lead or zinc oxide, bring two advantages, the first one is lead-free composition and the second one is that barium phosphate glasses are generally more chemically, thermally and mechanically durable than zinc phosphate glasses [14].

Experimental

Glasses of the $\text{BaO}-\text{P}_2\text{O}_5-\text{WO}_3$ system were prepared from reagent grade BaCO_3 , H_3PO_4 and WO_3 in batches of 25 g. The homogenized starting mixtures were slowly calcined up to 600 °C with the final calcination at the maximum temperature for 2 h in order to remove the water. The reaction mixtures were then melted at 1000–1150 °C under ambient air, in a platinum crucible. The melt was subsequently poured into a preheated graphite mold ($T < T_g$), and the obtained glass was then cooled to room temperature. The amorphous character of the prepared glasses was checked by X-ray diffraction analysis (not shown).

The elemental analysis of the bulk glasses was studied using scanning electron microscope LYRA 3 (Tescan) equipped with EDS analyzer AZtec X-Max 20 (Oxford Instruments). The EDS measurement was taken at 20 kV acceleration voltage on two $400 \times 400 \mu\text{m}$ spots. Transmittance spectra in the UV, visible and near-infrared range were obtained between 200 and 2000 nm using a spectrophotometer Shimadzu UV-3600 on polished glassy samples.

The glass density, ρ , was determined on bulk samples by the Archimedes method using toluene as the immersion liquid. The molar volume, V_M , was calculated using the expression $V_M = \bar{M}/\rho$. Density of polycrystalline sample was determined using a helium gas pycnometer AccuPyc II 1340, whereby the volume of the sample was measured by measuring the volume of the helium gas displaced by the sample.

Chemical durability of glasses was evaluated from their dissolution rate in distilled water at 25 °C. Glass cubes were placed in 100 cm^3 of water for 7 days. The dissolution rate, DR, was calculated from the expression $\text{DR} = \Delta\omega/S_t$, where $\Delta\omega$ is the mass loss (g), S is the sample area (cm^2) before the dissolution test and t is the dissolution time (min).

Thermal behavior of the glasses was studied with the DTA 404 PC (Netzsch) operating in the heat flux DSC mode at a heating rate of $10 \text{ }^\circ\text{C min}^{-1}$ over the temperature range 30–1000 °C. The measurements were taken with 100 mg powder samples in a silica crucible under an inert atmosphere of N_2 . The thermal expansion coefficient, α , the glass transition temperature, T_g , and the dilatometric softening temperature, T_d , were measured on bulk samples with dimensions of $20 \times 5 \times 5 \text{ mm}$ using a dilatometer DIL 402 PC (Netzsch). From the obtained dilatometric curves, the coefficient of thermal expansion, α , was determined as the mean value in the temperature range of 100–200 °C, the glass transition temperature, T_g , was determined from the change in the slope of the elongation versus temperature plot and dilatometric softening temperature, T_d , was determined as the maximum of the expansion trace corresponding to the onset of viscous deformation. The dilatometric measurements were taken in the air at a heating rate of $5 \text{ }^\circ\text{C min}^{-1}$. The thermal properties were also studied with hot-stage microscopy (HSM) from HESSE GmbH, which was carried out with powder samples pressed into cylinders (3 mm in diameter and height) with a hand press. The specimen was placed on a corundum sample holder, and the measurement was taken with a heating rate of $5 \text{ }^\circ\text{C min}^{-1}$ from room temperature to melting point under a static air atmosphere. The projected area and the height of the pressed powder sample were monitored with a CCD camera during the heating.

A Bruker D8 Advance diffractometer with CuK_α radiation was used for the identification of crystalline phases. A database of inorganic compounds from International Center of Diffraction Data [15] was used for the phase identification.

Raman spectra in the range $1400\text{--}200 \text{ cm}^{-1}$ were measured on glassy bulk and crystalline powder samples at room temperature using a DXR Raman spectrometer (Thermo Scientific) with a 532 nm solid-state (Nd:YAG) diode pumped laser.

^{31}P MAS NMR spectra were measured at 9.4 T on a BRUKER Avance 400 spectrometer with a 4 mm probe. The spinning speed was 12.5 kHz, and relaxation (recycling) delay was 180 s, which was enough to enable relaxation for quantitative analysis. The chemical shifts of ^{31}P nuclei are given relative to H_3PO_4 at 0 ppm.

Results and discussion

Physico-chemical and thermal properties

We have prepared seven samples of $(100 - x)\text{Ba}(\text{PO}_3)_2 - x\text{WO}_3$ glasses with 0, 10, 20, 30, 40, 50 and 60 mol% WO_3 by the procedure described above. Their compositions

(shown in Table 1) were checked by EDS analysis (determined values are also provided in Table 1). The analyzed compositions were found to be very close to the nominal compositions. The starting barium metaphosphate glass was colorless, while the color of barium tungstate-phosphate glasses changed from light blue to dark blue with increasing WO₃ content. This coloration is caused by absorption of visible light by the present W⁵⁺ species [8, 16, 17]. The presence of this species was confirmed by UV-VIS-NIR spectroscopy, and the transmittance spectra of the glasses with $x = 0$ –40 WO₃ are shown in Fig. 1. The spectrum of the parent glass 50BaO–50P₂O₅ exhibits short-wavelength absorption edge shifted deep in the UV region, while the WO₃-containing glasses reveal short-absorption edge shifted significantly toward the visible region (see Fig. 1). Spectra of glasses containing WO₃ reveal a strong absorption within the spectral range 580–820 nm for the glass with $x = 10$. This absorption becomes broader with increasing WO₃ content and the sample with $x = 40$ is almost broad enough to prevent transmission of visible light, which results in dark-colored samples. The absorption of the visible light by the reduced species can occur both by electronic d - d transitions (at 600 nm) and by polaron absorption between reduced and oxidized species [17] (at 850 nm), in this case between W⁵⁺ and W⁶⁺ species.

The values of density and molar volume of the studied glasses are provided in Table 2. The density monotonously increases with increasing WO₃ content, whereas molar volume decreases. The increase in density is caused by the replacement of BaO and P₂O₅ by heavier WO₃, whereas molar volume decreases due to the replacement of nine atoms of P₂O₅ and BaO by only four atoms of WO₃. The study of chemical durability showed that the dissolution rate for the WO₃-containing glasses is very small. The mass changes in the WO₃-containing glassy samples after their interaction with distilled water at room temperature for 7 days were a few tenths of milligram, which are the values within the measurement error. From these studies, we have estimated that the dissolution rate varies within the values of 1.4×10^{-8} – 6.2×10^{-9} g cm⁻² min⁻¹.

Table 1 Batched and analyzed compositions of (100 - x)Ba(PO₃)₂- x WO₃ glasses by SEM-EDS

Sample	Batched composition/mol%			Analyzed composition/mol%		
	BaO	WO ₃	P ₂ O ₅	BaO ± 0.2	WO ₃ ± 0.2	P ₂ O ₅ ± 0.3
$x = 0$	50	0	50	50.4	0	49.6
10	45	10	45	44.9	10.3	44.8
20	40	20	40	39.8	20.5	39.7
30	35	30	35	34.7	30.7	34.6
40	30	40	30	29.9	40.6	29.5
50	25	50	25	24.7	50.5	24.8
60	20	60	20	19.5	60.6	19.9

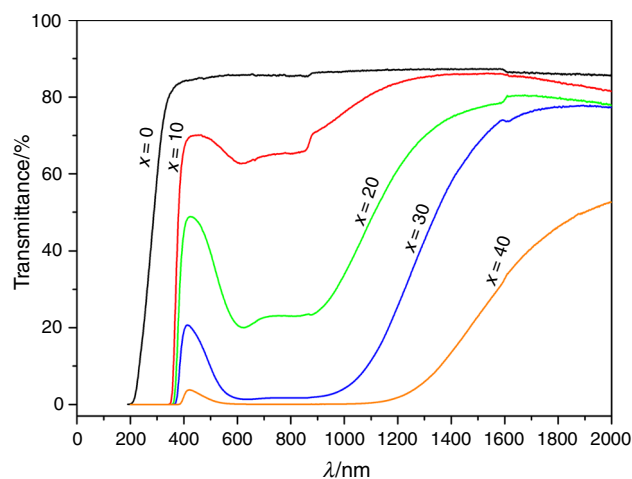


Fig. 1 UV-VIS-NIR transmittance spectra of (100 - x)Ba(PO₃)₂- x WO₃ glasses

DTA curves of (100 - x)Ba(PO₃)₂- x WO₃ glasses are shown in Fig. 2. As can be seen from this figure, almost all glasses reveal pronounced exothermic crystallization peaks, with the exception of the glasses with $x = 20$ –30 mol% WO₃. In the high-temperature region, we can also observe endothermic peaks corresponding to the melting of crystalline phases. The values of the glass transition temperature, T_g , determined from DTA curves as the onset of the change in the heat capacity, and the crystallization temperature, T_c , determined from these curves as the onset of crystallization peaks, are given in Table 2. In Table 2, the values of the difference ($T_c - T_g$) are also given, which serve often as a simple criterion of thermal stability of glasses. We can see that these values increase with increasing WO₃ content within the range 0–10 mol% WO₃; for the thermally stable glasses with 20 and 30 mol% without crystallization peak T_c values could not be determined, and then for the glasses with 40–60 mol% the difference ($T_c - T_g$) decreases.

The compositional dependences of the glass transition temperature, T_g , dilatometric softening temperature, T_d , and the coefficient of thermal expansion, α , of (100 - x)Ba(PO₃)₂- x WO₃ glasses, obtained from

Table 2 Composition, density, ρ , molar volume, V_M , dissolution rate, DR, glass transition temperature, T_g , crystallization temperature, T_c , criterion of thermal stability of glasses, $T_c - T_g$, and flow temperature, T_f , of $(100 - x)\text{Ba}(\text{PO}_3)_2 - x\text{WO}_3$ glasses

BaO mol%	WO ₃	P ₂ O ₅	$\rho \pm 0.02$ g cm ⁻³	$V_M \pm 0.5$ cm ³ mol ⁻¹	DR ± 0.2 g cm ⁻² min ⁻¹	$T_g \pm 2$ °C	$T_c \pm 2$ °C	$T_c - T_g$ °C	$T_f \pm 2$ °C
50	0	50	3.64	40.6	$1.8 \cdot 10^{-7}$	461	536	75	870
45	10	45	3.89	40.1	$1.5 \cdot 10^{-8}$	482	643	161	808
40	20	40	4.18	39.4	$1.4 \cdot 10^{-8}$	499	–	–	777
35	30	35	4.48	38.6	$6.2 \cdot 10^{-9}$	542	–	–	841
30	40	30	4.88	37.4	$3.0 \cdot 10^{-8}$	595	732	137	907
25	50	25	5.16	36.8	$2.4 \cdot 10^{-8}$	605	734	129	940
20	60	20	5.47	36.2	$2.2 \cdot 10^{-8}$	623	726	103	991

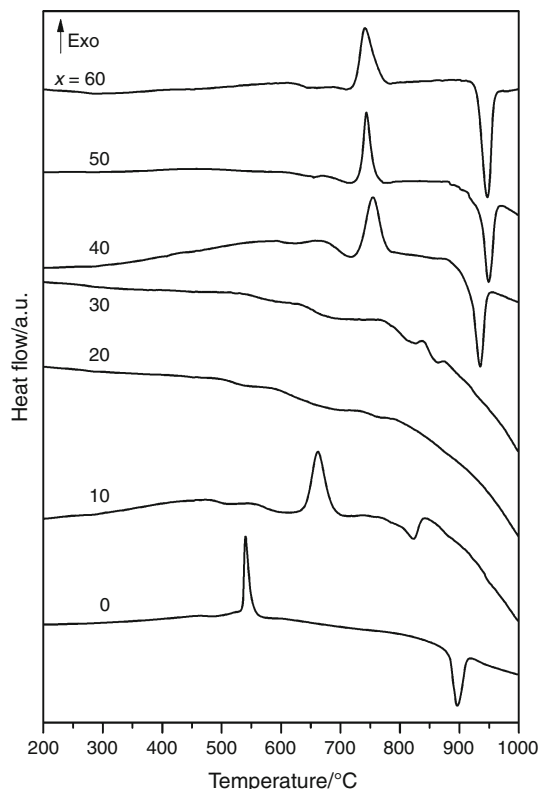


Fig. 2 DTA curves of the $(100 - x)\text{Ba}(\text{PO}_3)_2 - x\text{WO}_3$ glasses

dilatometric measurements, are shown in Fig. 3. The glass transition temperature increases from 463 °C, for the starting barium metaphosphate glass, up to 639 °C for the glass with 60 mol% of WO₃. A similar trend was also observed for the dilatometric softening temperature. The coefficient of thermal expansion reveals the opposite trend, it decreases from 14.7 ppm °C⁻¹ down to 9.2 ppm °C⁻¹ for the sample with $x = 50$ mol% WO₃.

Generally, T_g of oxide glasses increases with the increasing bond strength, cross-link density and closeness of packing of the glass structure. Since the energy of W–O bonds ($E_{\text{W-O}} = 672.0 \pm 20.9$ kJ mol⁻¹ [18]) is higher than the energy of P–O bonds ($E_{\text{P-O}} = 599.1 \pm 12.6$ kJ mol⁻¹ [18]) and the energy of Ba–O bonds ($E_{\text{Ba-O}} = 561.9 \pm 13.4$ kJ mol⁻¹ [18]), the mean bond strength

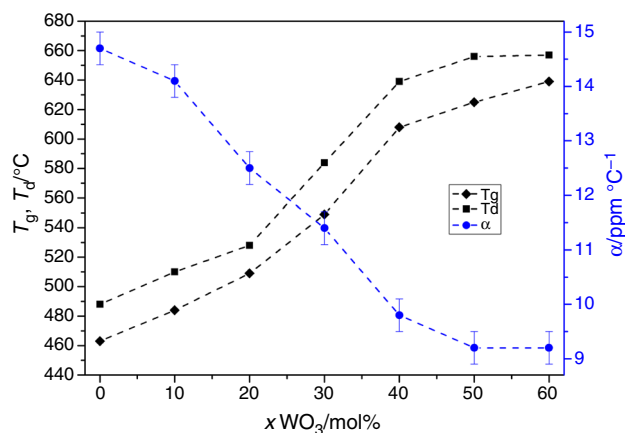


Fig. 3 Compositional dependence of the glass transition temperature, T_g , dilatometric softening temperature, T_d and the coefficient of thermal expansion, α , in the glass series $(100 - x)\text{Ba}(\text{PO}_3)_2 - x\text{WO}_3$. The error in the values of T_g is smaller than the symbol size. The lines are only a guide to the eye

increases with an increase in the WO₃ content. The values of T_g , determined from dilatometric curves, are slightly higher than those determined from DTA curves.

The thermoanalytical curves from hot-stage microscopy of $(100 - x)\text{Ba}(\text{PO}_3)_2 - x\text{WO}_3$ glasses reveal the temperature dependence of the projected area and the height of the pressed powder sample (Fig. 4). The first dimensional changes are related to T_g , when the decreasing viscosity of the glass results in a shrinkage of the sample. We used this first dimensional change for the verification of the determined glass transition temperature for the glasses having small changes in the thermal capacity c_p in the glass transformation region. Crystallization of the glass renders a decrease in the glass viscosity similar to the starting glass $50\text{BaO} - 50\text{P}_2\text{O}_5$ ($x = 0$), and thus, the HSM curve reveals a plateau until the melting temperature of the crystallized glass (876 °C from DTA, Fig. 2). It is evident that most glasses reveal these crystallization plateaus. From the HSM measurement, we have also determined the values of the flow temperature, T_f , given in Table 2. The flow temperature, T_f , is the first temperature at which the sample is melted to a third of its original height [19]. These values

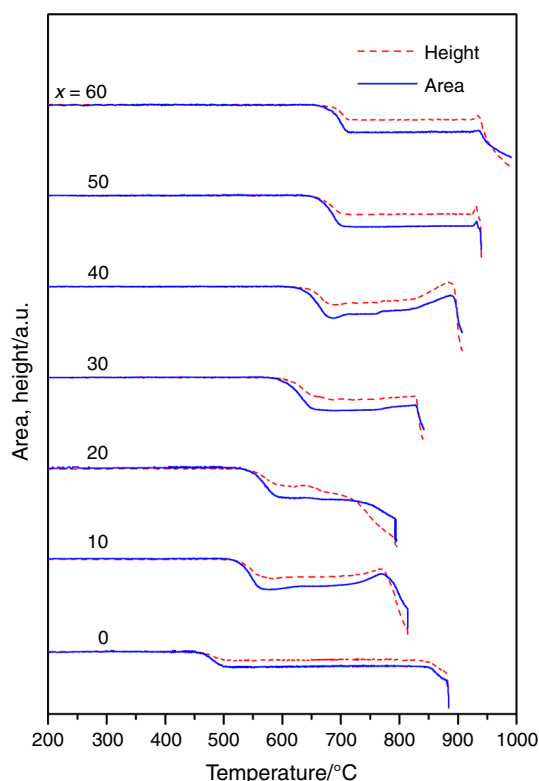


Fig. 4 Hot-stage microscopy of the $(100 - x)\text{Ba}(\text{PO}_3)_2 - x\text{WO}_3$ glasses

show a minimum for the sample with 20 mol% WO₃ which reveals the highest thermal stability.

Glass crystallization and glass-to-crystal transformation

We have also studied crystallization products obtained by annealing glass powders at the temperatures above their crystallization peaks on the DTA curves. The annealing temperatures and times are provided in Table 2 along with the compositions of crystalline products identified by X-ray diffraction analysis with the application of database PDF-4 [15]. We have to apply longer annealing times (16 h) for the glasses with $x = 20$ – 30 mol% WO₃ due to a smaller tendency of these glasses toward crystallization. The diffraction patterns of the crystalline phases are given in Fig. 5. Even with that, we did not succeed in obtaining fully crystallized samples (this is noticeable in Fig. 5 for the sample with $x = 20$ due to the presence of the halo centered at $2\theta = 25^\circ$). Altogether, three crystalline phases were identified in the diffraction patterns (see Table 3), but one of them could not be found in the database of inorganic compounds [15]. This unknown phase was detected in the samples with $x = 20$ – 60 mol% WO₃, but only for the samples with 40 and 50 mol% WO₃ it was represented as the only one.

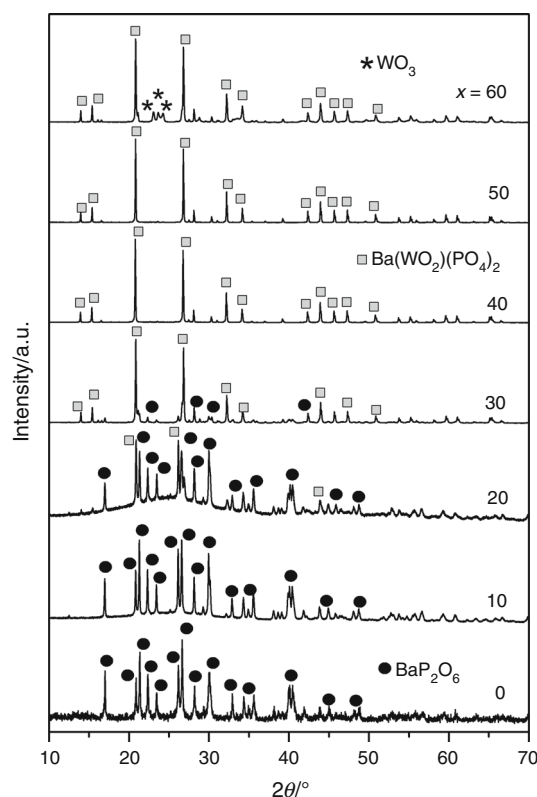


Fig. 5 XRD patterns of crystallized samples of the $(100 - x)\text{Ba}(\text{PO}_3)_2 - x\text{WO}_3$ glasses

Table 3 Composition, annealing temperatures, T_a , annealing times, t_a , and crystallization products of $(100 - x)\text{Ba}(\text{PO}_3)_2 - x\text{WO}_3$ glasses

BaO mol%	WO ₃	P ₂ O ₅	T_a °C	t_a h	Products of crystallization
50	0	50	600	6	BaP ₂ O ₆
45	10	45	690	6	BaP ₂ O ₆
40	20	40	620	16	BaP ₂ O ₆ , Ba(WO ₂) ₂ (PO ₄) ₂
35	30	35	680	16	BaP ₂ O ₆ , Ba(WO ₂) ₂ (PO ₄) ₂
30	40	30	780	6	Ba(WO ₂) ₂ (PO ₄) ₂
25	50	25	800	6	Ba(WO ₂) ₂ (PO ₄) ₂
20	60	20	770	6	WO ₃ , Ba(WO ₂) ₂ (PO ₄) ₂

Previous studies of crystallization of various ternary systems with MoO₃ or WO₃ revealed that in several ternary systems, a crystalline compound is formed at the composition of 25MO(M₂O)-50MoO₃(WO₃)-25P₂O₅. In the ternary system PbO-MoO₃-P₂O₅, the crystalline phase of the composition Pb(MoO₂)₂(PO₄)₂ [20] was identified; similarly in the BaO-MoO₃-P₂O₅ system, Ba(MoO₂)₂(PO₄)₂ compound was found [21]. In the Ag₂O-MoO₃-P₂O₅ system AgMoO₂PO₄ compound [7, 22] and in PbO-WO₃-P₂O₅ system Pb(WO₂)₂(PO₄)₂ compound [23] were studied. In the

ternary systems $\text{Na}_2\text{O}-\text{WO}_3/\text{MoO}_3-\text{P}_2\text{O}_5$, similar compounds $\text{NaMoO}_2\text{PO}_4/\text{NaMoO}_2\text{PO}_4$ were prepared and studied [24, 25]. That is why we assumed, that in our case, a crystalline phase of the composition $\text{Ba}(\text{WO}_2)_2(\text{PO}_4)_2$ is formed. Also, the X-ray diffraction patterns of $\text{Ba}(\text{WO}_2)_2(\text{PO}_4)_2$ compound reveal very similar diffraction lines to crystalline phases mentioned above. The obtained diffractogram (Fig. 5) from our crystallized sample contains 75 sharp diffraction lines with FWHM of approximately $0.07^\circ 2\Theta$, which suggest a hexagonal cell of dimensions $a = 11.5191(1) \text{ \AA}$ and $c = 6.3437(1) \text{ \AA}$ with figures of merit $M(20) = 298$ [26] and $F(20) = 420 (0.0018, 26)$ [27]. No systematic absences of hkl reflections were observed. Twenty possible space groups were found by means of the CHECKCELL program [28]. The volume of elemental cell is $728.97(2) \text{ \AA}^3$, and we assume the unit cell contains three formulae $\text{Ba}(\text{WO}_2)_2(\text{PO}_4)_2$ ($M = 758.97$, $Z = 3$). In this case, the calculated density $D_x = 5.187 \text{ g cm}^{-3}$ is in good agreement with the experimental value of 5.240 g cm^{-3} . Full powder pattern is provided in supplementary file. From the DTA curve, we have also determined its melting point as $936 \text{ }^\circ\text{C}$.

Raman spectra of all thermal-treated samples of $(100 - x)\text{Ba}(\text{PO}_3)_2-x\text{WO}_3$ glasses are shown in Fig. 6. Samples containing 0–30 mol% WO_3 reveal sharp vibrational bands at $1156, 690, 402$ and 304 cm^{-1} , characteristic

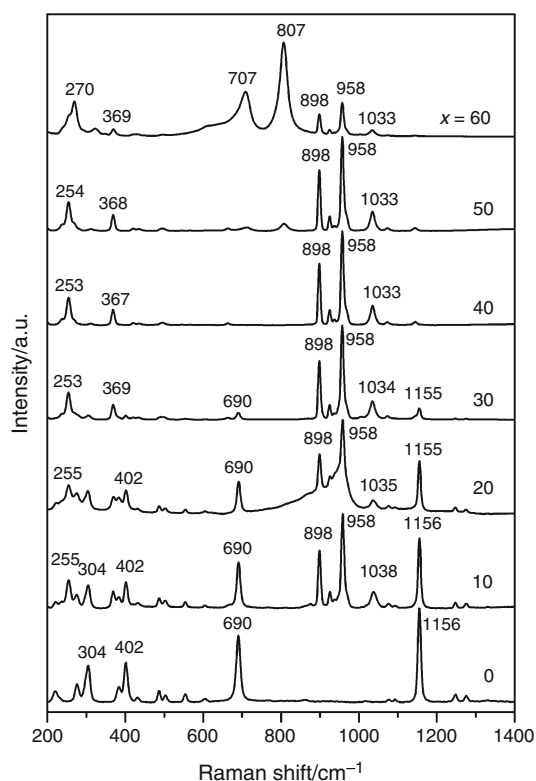


Fig. 6 Raman spectra of crystallized samples of the $(100 - x)\text{Ba}(\text{PO}_3)_2-x\text{WO}_3$ glasses

of the crystalline compound BaP_2O_6 . Their intensity decreases with the decreasing content of barium metaphosphate in the glasses. In the Raman spectra of glasses with 10–60 mol% WO_3 , we can observe vibrational bands at $1033, 958, 898, 367$ and 253 cm^{-1} which we ascribe to the ternary compound $\text{Ba}(\text{WO}_2)_2(\text{PO}_4)_2$ corresponding to the glass with 50 mol% WO_3 . In the thermal-treated sample with 60 mol% WO_3 , we can see in Fig. 6 also characteristic Raman bands of the tungsten trioxide WO_3 [29] at $807, 707$ and 270 cm^{-1} . In this way, the Raman spectra of the thermal-treated samples are in good agreement with the results obtained by X-ray diffraction analysis in terms of identified crystalline phases (Table 3). However, Raman spectra show also the presence of the glass-crystalline state at the thermal-treated sample with 20 mol% WO_3 , where we can observe also the presence of a wide vibrational band in the range of $800-1000 \text{ cm}^{-1}$, which confirms its extra thermal stability in agreement with the results of DTA analysis (see Fig. 2).

We have also recorded the ^{31}P MAS NMR spectrum of the polycrystalline $\text{Ba}(\text{WO}_2)_2(\text{PO}_4)_2$ compound and plotted it together with the spectrum of the corresponding glass as shown in Fig. 7. The presence of only one signal in the ^{31}P MAS spectrum (at -4 ppm) reveals only one phosphorus local environment in this compound. A broad NMR signal shows the presence of two or three different Q^n units in the glass structure at this composition.

Raman spectra of the polycrystalline $\text{Ba}(\text{WO}_2)_2(\text{PO}_4)_2$ compound and the corresponding glass are shown in Fig. 8. We can see some similarities between Raman spectra of the glass and crystal, but also some differences. The main difference is the absence of the strong vibrational band in the crystalline compound, which would correspond to the broadband of 834 cm^{-1} in the Raman spectrum of the glass

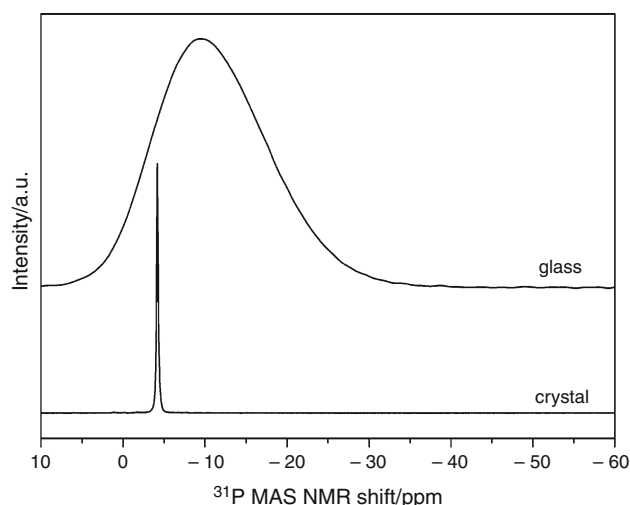


Fig. 7 ^{31}P MAS NMR spectra of $25\text{BaO}-50\text{WO}_3-25\text{P}_2\text{O}_5$ glass and the corresponding polycrystalline compound $\text{Ba}(\text{WO}_2)_2(\text{PO}_4)_2$

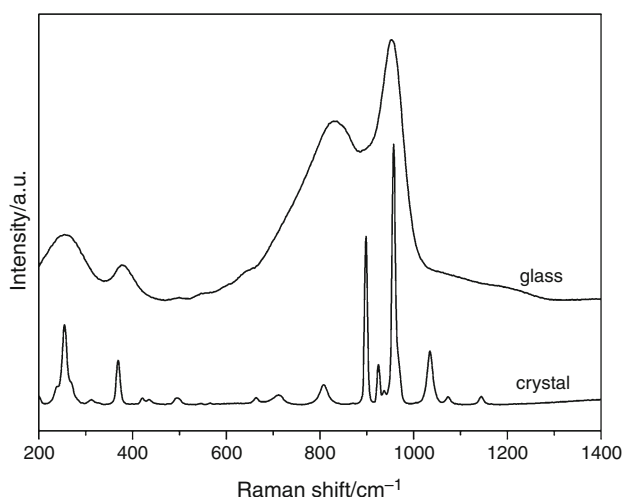


Fig. 8 Raman spectra of 25BaO-50WO₃-25P₂O₅ glass and the corresponding polycrystalline compound Ba(WO₂)₂(PO₄)₂

samples. Because this band in the glass is ascribed to the W–O–W linkages connecting WO₆ octahedra, we can consider the absence of W–O–W connections in the crystalline Ba(WO₂)₂(PO₄)₂ compound like in the NaWO₂PO₄ compound [24]. The dominant band of 955 cm⁻¹ in the Raman spectrum of glass ascribed to stretching vibrations of W–O bond can have similar assignment also in the crystalline compound similar to the Raman spectrum of the W₂O₃(PO₄)₂ measured by Kim and Condrate [30]. Vibrational band of 368 cm⁻¹, ascribed in the tungsten phosphate glasses to P–O–W vibrations [31], has a similar vibrational band in the spectrum of the polycrystalline compound.

Conclusions

We have found that tungsten oxide WO₃ is able to form glasses with barium metaphosphate Ba(PO₃)₂ in a broad range of 0–60 mol% WO₃. The combination of BaO and WO₃ contributes to very high chemical durability of glasses and to very high glass transition temperatures of WO₃-rich glasses above 600 °C. Crystallization of glasses revealed the formation of the Ba(WO₂)₂(PO₄)₂ compound in the Ba(PO₃)₂-WO₃ series. We were able to determine the parameters of its elementary cell and its melting point. We suppose that its structure will have similar basic structural units as previously studied compounds, i.e., PO₄ tetrahedra and WO₆ octahedra. Comparison of the Raman spectra of polycrystalline compound and the glass of the same composition supports this conclusion.

Acknowledgements The Czech authors are grateful for the financial support from the Project No. 18-01976S of the Grant Agency of the Czech Republic. EDS measurements were taken with the support of

the Grants LM2015082 and ED4.100/11.0251 provided by the MSM T Czech Republic. The authors thank L. Montagne and B. Revel for the ³¹P MAS NMR spectra of the polycrystalline Ba(WO₂)₂(PO₄)₂ compound and the corresponding glass of the same composition.

References

- Brow RK. Review: the structure of simple phosphate glasses. *J Non-Cryst Solids*. 2000;263–264:1–28.
- Hsu SM, Wu JJ, Yung SW, Chin TS, Zhang T, Lee YM, Chu CM, Ding JY. Evaluation of chemical durability, thermal properties and structure characteristics of Nb–Sr–phosphate glasses by Raman and NMR spectroscopy. *J Non-Cryst Solids*. 2012;358:14–9.
- Pinet O, Dussossoz JL, David C, Fillet C. Glass matrices for immobilizing nuclear waste containing molybdenum and phosphorus. *J Nucl Mater*. 2008;377:307–12.
- Granqvist CG. Electrochromic tungsten oxide films: review of progress 1993–1998. *Sol Energy Mater Sol Cells*. 2000;60:201–62.
- Porier G, Nalin M, Messaddeq Y, Ribeiro SJL. Photochromic properties of tungstate-based glasses. *Solid State Ion*. 2007;178:871–5.
- de Araujo CC, Strojek W, Zhang L, Eckert H, Poirier G, Ribeiro SJL, Messaddeq Y. Structural studies of NaPO₃-WO₃ glasses by solid state NMR and Raman spectroscopy. *J Mater Chem*. 2006;16:3277–84.
- Santagneli SH, Poirier G, Rinke MT, Ribeiro SJL, Messaddeq Y, Eckert H. Structural investigations of tungsten silver phosphate glasses by solid state NMR, vibrational and X-ray absorption near edge spectroscopies. *J Non-Cryst Solids*. 2011;357:2126–31.
- Bih L, Abbas L, Azrou M, El Amraoui Y, Nadiri A. EPR investigation and thermal study of yA₂O–(1–y)[0.25(WO₃)₂–0.75(P₂O₅)] (A = Li, Na) glasses. *J Therm Anal*. 2005;81:57–60.
- Manzani D, Fernandes RG, Messaddeq Y, Ribeiro SJL, Cassanjes FC, Poirier G. Thermal, structural and optical properties of new tungsten lead-pyrophosphate glasses. *Opt Mater*. 2011;33:1862–6.
- Bih L, Abbas L, Mohdachi S, Nadiri A. Thermal and electrical properties of mixed alkali in Li₂O–Na₂O–WO₃–P₂O₅ glasses. *J Mol Struct*. 2008;891:173–7.
- Subbalakshmi P, Veeraiah N. Study of CaO–WO₃–P₂O₅ glass system by dielectric properties. IR spectra and differential thermal analysis. *J Non-Cryst Solids*. 2002;298:89–98.
- Kuzmin A, Purans J. X-ray absorption study of the short range order of tungsten and molybdenum ions in BaO–P₂O₅–WO₃ and CaO–P₂O₅–MoO₃ glasses. *Journal de Physique IV Colloque*. 1997;7:971–3.
- Marzouk MA, ElBatal FH, Ghoneim NA, Ezz-Eldin FM. Optical, FTIR and ESR spectral investigations of tungsten ions in barium phosphate host glass and effects of gamma irradiation. *Silicon*. 2018;10:959–65.
- Jung BH, Kim DK, Kim HS. Properties and structure of (50 – x)BaO–xZnO–50P₂O₅. *J Non-Cryst Solids*. 2005;351:3356–60.
- Joint Committee on powder diffraction standards, Swarthmore, PA, USA. International Centre of Diffraction Data.
- Tawarazama H, Utsuno F, Inoue H, Hosono H, Kawayoe H. Coloration and decoloration of tungsten phosphate glasses by heat treatments at the temperature far below T_g under a controlled ambient. *Chem Mater*. 2006;18:2810–6.
- Porier G, Ottoboni FS, Cassanjes FC, Remonte Á, Messaddeq Y, Ribeiro SJL. Redox behavior of molybdenum and tungsten in phosphate glasses. *J Phys Chem B*. 2008;112:4481–7.
- Lide DR. Handbook of chemistry and physics. Boca Raton: CRC Press; 2001. p. 9–52.

19. Mošner P, Vorokhta M, Koudelka L. Application of heating microscopy to the study of thermal behaviour of ZnO–P₂O₅–WO₃ glasses. *J Therm Anal Calorim.* 2013;112:659–64.
20. Rösslerová I, Koudelka L, Černošek Z, Mošner P, Beneš L. Thermal properties and crystallization of PbO–MoO₃–P₂O₅ glasses. *J Mater Sci.* 2011;46:6751–7.
21. Kalenda P, Koudelka L, Mošner P, Beneš L, Černošek Z. Thermal properties and crystallization of BaO–MoO₃–P₂O₅ glasses. *J Therm Anal Calorim.* 2018;131:2303–10.
22. Kierkegaard P, Holmen S. The crystal structure of AgMoO₂PO₄. *Ark Kemi.* 1965;23:213–21.
23. Rösslerová I, Koudelka L, Černošek Z, Mošner P, Beneš L. Study of crystallization of PbO–WO₃–P₂O₅ glasses by thermoanalytical and spectroscopic methods. *J Non-Cryst Solids.* 2014;384:41–6.
24. Kierkegaard P. The crystal structure of NaMoO₂PO₄ and NaWO₂PO₄. *Ark Kemi.* 1961;18:553–75.
25. Koudelka L, Kupetska O, Kalenda P, Mošner P, Montagne L, Revel B. Crystallization of sodium molybdate–phosphate and tungstate–phosphate glasses. *J Non-Cryst Solids.* 2018;500:42–8.
26. de Wolff PM. A simplified criterion for the reliability of a powder pattern indexing. *J Appl Crystallogr.* 1968;1:108–13.
27. Smith GS, Snyder RL. FN: a criterion for rating powder diffraction patterns and evaluating the reliability of powder-pattern indexing. *J Appl Crystallogr.* 1979;12:60–5.
28. Laugier J, Bochu B. LMGP-Suite, ENSP/Laboratoire des Matériaux et du Genie Physique, Saint Martin d’Heres, France. <http://www.inpg.fr/LMGP> and <http://www.ccp14.ac.uk/tutorial/lmgp/>. Accessed Aug 2018.
29. Boulova M, Lucazeau G. Crystallite nanosize effect on the structural transitions of WO₃ studied by Raman spectroscopy. *J Solid State Chem.* 2002;167:425–34.
30. Kim CY, Condrate RA Sr. The vibrational spectra of crystalline W₂O₃(PO₄)₂ and related tungsten phosphate glasses. *J Phys Chem Solids.* 1984;45:1213–8.
31. Šubčík J, Koudelka L, Mošner P, Gregora I, Montagne L, Delevoye L. Glass-forming ability and structure of glasses in the ZnO–WO₃–P₂O₅ system. *Phys Chem Glasses Part B.* 2012;53:79–85.

Publisher’s Note Springer Nature remains neutral with regard to jurisdictional claims in published maps and institutional affiliations.